We can conclude the following. From $\nu_k^\star = \lambda > 0$, $k = 1, \ldots, K$, it follows that the corresponding constraints are tight, i.e., $\mathrm{tr}(\mathbf{Q}_k^\star) = p_k^\star$. Furthermore, $\mathbf{\Gamma}^\star = \mathbf{W}^{\star-1} \succ 0$ implies that the corresponding constraint is tight, i.e., $\mathbf{W}^\star = \sum_{k=1}^K \tilde{\mathbf{H}}_k \mathbf{Q}_k^\star \tilde{\mathbf{H}}_k^H + \mathbf{I}$. This confirms the equivalence of problems (4) and (6) and implies that $\mathbf{\Gamma}^\star = (\sum_{k=1}^K \tilde{\mathbf{H}}_k \mathbf{Q}_k^\star \tilde{\mathbf{H}}_k^H + \mathbf{I})^{-1}$ and

$$\tilde{\mathbf{H}}_k^h \left(\sum_{k=1}^K \tilde{\mathbf{H}}_k \mathbf{Q}_k^\star \tilde{\mathbf{H}}_k^H + \mathbf{I} \right)^{-1} \tilde{\mathbf{H}}_k = \lambda \mathbf{I} - \mathbf{\Psi}_k^\star, \qquad k = 1, \ldots, K. \tag{21}$$

The last equation is very similar to the single user WF condition. The only difference is that λ (i.e., the inverse of the water level) is not obtained from a sum power constraint. It is a fixed value so that it determines the sum power by itself. Since $\mathbf{\Psi}_k^\star \succeq 0$, from (21), it follows that $\lambda_{\max}(\{\mathbf{Q}_k^\star\})$, which is defined in (15), satisfies

$$\bar{\lambda}(\{\mathbf{Q}_k^\star\}) = \begin{cases} \lambda_0 < \lambda, & \text{if } \mathbf{\Psi}_k^\star \succ 0 \quad \text{for all } k = 1, \ldots, K \\ \lambda, & \text{otherwise.} \end{cases} \tag{22}$$

From the complementary slackness, i.e., $\mathrm{tr}(\mathbf{\Psi}_k^\star \mathbf{Q}_k^\star) = 0$, it follows that $\mathbf{\Psi}_k^\star \succ 0$ for all $k = 1, \ldots, K$ implies that $\mathbf{Q}_k^\star = 0$ for all $k = 1, \ldots, K$. By letting $\mathbf{Q}_k^\star = 0$ in (21), it is easy to observe that $\mathbf{\Psi}_k^\star \succ 0$ if and only if $\lambda > \lambda_{\max}(\tilde{\mathbf{H}}_k^H \tilde{\mathbf{H}}_k)$ for all $k = 1, \ldots, K$. Physically, this situation corresponds to a very small water level in (21), which does not inundate any of the channel eigenmodes. Clearly, such λ values cannot be optimal for master problem (5). Thus, the search domain of master problem (5) can be restricted to $\lambda < \max_{k=1, \ldots, K} \lambda_{\max}(\tilde{\mathbf{H}}_k^H \tilde{\mathbf{H}}_k)$. In such conditions, $\bar{\lambda}(\{\mathbf{Q}_k^\star\}) = \lambda$, and therefore, the dual variable that is defined in (16) become an optimal dual variable, i.e., $\bar{\mathbf{\Gamma}}(\{\mathbf{Q}_k^\star\}) = (\sum_{k=1}^K \hat{\mathbf{H}}_k \mathbf{Q}_k^\star \hat{\mathbf{H}}_k^H + \mathbf{I})^{-1} = \mathbf{\Gamma}^\star$.

REFERENCES

[1] S. Vishwanath, N. Jindal, and A. Goldsmith, "Duality, achievable rates, and sum-rate capacity of Gaussian MIMO broadcast channels," *IEEE Trans. Inf. Theory*, vol. 49, no. 10, pp. 2658–2668, Oct. 2003.

[2] P. Viswanath and D. N. C. Tse, "Sum capacity of the vector Gaussian broadcast channel and uplink–downlink duality," *IEEE Trans. Inf. Theory*, vol. 49, no. 8, pp. 1912–1921, Aug. 2003.

[3] W. Yu and J. M. Cioffi, "Sum capacity of Gaussian vector broadcast channels," *IEEE Trans. Inf. Theory*, vol. 50, no. 9, pp. 1875–1892, Sep. 2004.

[4] H. Viswanathan, S. Venkatesan, and H. Huang, "Downlink capacity evaluation of cellular networks with known interference cancellation," *IEEE J. Sel. Areas Commun.*, vol. 21, no. 5, pp. 802–811, Jun. 2003.

[5] W. Yu, "A dual decomposition approach to the sum power Gaussian vector multiple access channel sum capacity problem," in *Proc. CISS*, Baltimore, MD, Mar. 12–14, 2003.

[6] N. Jindal, W. Rhee, S. Vishwanath, S. A. Jafar, and A. Goldsmith, "Sum power iterative water-filling for multi-antenna Gaussian broadcast channels," *IEEE Trans. Inf. Theory*, vol. 51, no. 4, pp. 1570–1580, Apr. 2005.

[7] M. Codreanu, M. Juntti, and M. Latva-aho, "Low complexity iterative algorithm for finding the MIMO-OFDM broadcast channel sum capacity," *IEEE Trans. Commun.*, vol. 55, no. 1, pp. 48–53, Jan. 2007.

[8] W. Yu, "Sum-capacity computation for the Gaussian vector broadcast channel via dual decomposition," *IEEE Trans. Inf. Theory*, vol. 52, no. 2, pp. 754–759, Feb. 2006.

[9] W. Yu, W. Rhee, S. Boyd, and J. M. Cioffi, "Iterative water-filling for Gaussian vector multiple-access channels," *IEEE Trans. Inf. Theory*, vol. 50, no. 1, pp. 145–152, Jan. 2004.

[10] T. M. Cover and J. A. Thomas, *Elements of Information Theory*. New York: Wiley, 1991.

[11] S. Boyd and L. Vandenberghe, *Convex Optimization*. Cambridge, U.K.: Cambridge Univ. Press, 2004.

[12] W. Yu, private communication, 2006.

New Space–Time Trellis Codes for Two-Antenna Quasi-Static Channels

Yi Hong, *Member, IEEE*, and
Albert Guillén i Fàbregas, *Member, IEEE*

Abstract—New space–time trellis codes with four- and eight-level phase-shift keying (PSK) and 16-phase quadrature amplitude modulation (QAM) for two transmit antennas in slow-fading channels are presented in this paper. Unlike most of the codes that are reported in the literature, the proposed codes are specifically designed to minimize the frame error probability from a union-bound perspective. The performance of the proposed codes with various memory orders and receive antennas is evaluated by simulation. It is shown that the proposed codes outperform previously known codes in all studied cases.

Index Terms—Diversity, multi-input multi-output channels, multiple antennas, space–time codes, trellis codes.

I. INTRODUCTION

Space–time trellis codes (STTCs) were originally proposed in [1] to achieve both diversity and coding gains on multi-input–multi-output (MIMO) fading channels by combining coding over multiple transmit antennas with high-order signal constellations. Design guidelines based on minimum rank and determinant were proposed in [1], mainly based on worst-case PairWise Error Probability (PWEP) analysis. Ever since, multiple efforts have been dedicated to further maximize the coding gain using the same rank and determinant criteria [2], [3]. An improved determinant criterion that highlights the role of the Euclidean distance for systems with medium to large diversity order was presented in [4]. Depending on the diversity order of the system, rank and determinant or Euclidean distance criteria have been used in [5], [6] to construct four eight-level phase-shift keying (8-PSK) STTCs by exhaustive computer search.

A specific rank criterion was developed in [7] for the particular case of high-order signal constellations such as 16-phase quadrature amplitude modulation (16-QAM). The core of this criterion is a sufficient condition to select full-rank codes without resorting to exhaustive computer search. Unfortunately, the coding gain of the codes in [7] was not optimized. In [8], improved 16-QAM STTCs were found by optimizing the coding gain based on the Euclidean distance criterion. A common feature of all aforementioned code design criteria is to minimize the worst case PWEP. To further improve performance, Jung and Lee [9] introduce a code search method based on the distance spectrum of the code [10]. This method is then used to search a single four-state four-level phase-shift keying (4-PSK) STTC [9].

In this paper, we consider design guidelines that aim to minimize a truncated union bound on the frame error rate (FER) by taking into account the first three terms. The PWEP terms depend on the values of the determinants and the corresponding number of codewords. This is similar to the approach that was taken in [11], where the PWEP terms depend on the Euclidean distances for moderate diversity gains instead. In our design, we construct three complete sets of 4-PSK, 8-PSK, and 16-QAM STTCs for two transmit antennas over slow (quasi-static)-fading channels. Through simulations, it is shown that, in all cases, the new codes outperform previously known codes [1]–[8], [11].

The rest of this paper is organized as follows: Section II introduces the system model, and Section III reviews the code design criteria. Section IV introduces STTC encoder structures for phase-shift keying (PSK) and 16-QAM, respectively. In Section V, new 4-PSK, 8-PSK, and 16-QAM STTCs are presented together with the simulation results. Conclusions are finally drawn in Section VI.

Notation: T denotes transpose, and $\dagger$ denotes transpose conjugate. Superscripts I and Q denote the real and imaginary parts of a complex number. $\mathbb{Z}_m = \{0, 1, \ldots, m-1\}$ denote the ring of the integers modulo m, and $\mathbb{Z}_m[j]$ is the ring of Gaussian integers modulo m, where each element $z \in \mathbb{Z}_m[j]$ has $\{z = z^I + jz^Q : z^I, z^Q \in \mathbb{Z}_m\}$, $j = \sqrt{-1}$. Complex numbers are denoted by $\mathbb{C}$.

II. SYSTEM MODEL

We consider a quasi-static multiple-antenna fading channel with n_T transmit and n_R receive antennas, for which the received signal matrix $\mathbf{Y} \in \mathbb{C}^{n_R \times L}$ is given by

$$\mathbf{Y} = \sqrt{E_s}\mathbf{H}\mathbf{X} + \mathbf{N} \tag{1}$$

where L is the frame length; $\mathbf{X} = [\mathbf{x}_1, \ldots, \mathbf{x}_t, \ldots, \mathbf{x}_L] \in \mathbb{C}^{n_T \times L}$ is the transmitted signal matrix; $\mathbf{x}_t = [x_t^1, \ldots, x_t^{n_T}]^T \in \mathbb{C}^{n_T}$ is the signal vector at time $1 \leq t \leq L$; $\mathbf{H} = [\mathbf{h}_1, \ldots, \mathbf{h}_{n_T}] \in \mathbb{C}^{n_R \times n_T}$ is the channel matrix, which remains constant during a frame of L channel uses and varies from one frame to another independently; $\mathbf{N} \in \mathbb{C}^{n_R \times L}$ is a matrix of complex white Gaussian noise independent and identically distributed (i.i.d.) samples $\sim \mathcal{N}_\mathbb{C}(0, N_0)$; and E_s/N_0 is the average signal-to-noise ratio (SNR) per transmit antenna. The elements of $\mathbf{H}$ are assumed to be i.i.d. circularly symmetric Gaussian random variables $\sim \mathcal{N}_\mathbb{C}(0, 1)$. We assume perfect channel state information at the receiver. We assume discrete signal constellations, namely, $x_t^i \in \mathcal{X}$ for $1 \leq t \leq L$ and $1 \leq i \leq n_T$, where $\mathcal{X} \subseteq \mathbb{C}$ denotes the PSK or quadrature amplitude modulation (QAM) signal set. We will refer to a rate R space–time code $\mathcal{S} \subseteq \mathcal{X}^{n_T \times L}$ as the set of all 2^{LR} codewords.

III. ERROR PROBABILITY AND CODE DESIGN

Assuming that a codeword $\mathbf{X} \in \mathcal{S}$ is transmitted, the maximum-likelihood receiver might decide erroneously in favor of another codeword $\widehat{\mathbf{X}} \in \mathcal{S}$, depending on the fading or noise realizations. Following [1], we define $\mathbf{B} \triangleq \mathbf{X} - \widehat{\mathbf{X}}$ as the *codeword difference matrix* and $\mathbf{A} \triangleq \mathbf{B}\mathbf{B}^\dagger$ as the *codeword distance matrix*. Let now $d \triangleq \det(\mathbf{A}) = \prod_{k=1}^{r} \lambda_k$, where λ_k are the r nonzero eigenvalues of $\mathbf{A}$ and $\mathcal{D} = \{d \in \mathbb{R} : d = \det(\mathbf{A}), \forall \mathbf{X} \neq \widehat{\mathbf{X}} \in \mathcal{S}\}$ is the set of all possible determinants of the codeword distance matrix. Then, the union bound on the FER becomes [9], [10]

$$P_{\text{FER}} \leq \left(\sum_{d \in \mathcal{D}} \overline{N}(d) \, d^{-n_R}\right)\left(\frac{E_s}{N_0}\right)^{-rn_R} \tag{2}$$

where

$$\overline{N}(d) \triangleq \frac{1}{b^v} \sum_{p=p_{\min}}^{p_{\max}} \frac{N(d, p)}{(2)^{mp}} \tag{3}$$

is the spectrum term, m is the number of bits per symbol of the signal constellation, $p_{\min} = \lfloor v/b + 1\rfloor$ is the minimum length in trellis steps of simple error events [5] and $\lfloor x \rfloor$ denotes the largest integer that is smaller than or equal to x, $p_{\max}$ is the maximum allowed length of trellis paths [5], $N(d, p)$ is the number of error events of length p and determinant d, v is the *memory order* of the encoder, and $b = \log_2 M, \log_4 M$ for M-PSK and M-QAM, respectively (see [10] for details). If we further define

$$\eta(p_{\max}) \triangleq \frac{1}{b^v} \sum_{d \in \mathcal{D}} \left\{ \sum_{p=p_{\min}}^{p_{\max}} \frac{N(d, p)}{(2)^{mp}} \right\} d^{-n_R} \tag{4}$$

(2) becomes

$$P_{\text{FER}} \leq \eta(p_{\max})\left(\frac{E_s}{N_0}\right)^{-rn_R} \tag{5}$$

and we can now formulate the code design criteria.

1) *Diversity gain*: $\mathbf{A}$ has to be full rank for all pairs of codewords.
2) *Coding gain*: $\eta(p_{\max})$ has to be minimized over all the possible error events in the trellis diagram.

IV. STTC ENCODER

In this section, we introduce two different STTC encoder structures for PSK and QAM, respectively.

A. M-PSK STTC Encoder

We consider the M-PSK STTC encoder with memory order v and n_T transmit antennas shown in Fig. 1(a). The M-PSK STTC encoder consists of an m-branch shift register with total memory order v. At time t, m binary inputs c_t^i, $i = 1, 2, \ldots, m$, are fed into the m branches. The memory order of the ith branch v_i is given by

$$v_i = \left\lfloor \frac{v + i - 1}{b} \right\rfloor \tag{6}$$

where $v = \sum_i v_i$.

The m streams of input bits are simultaneously passed through their respective shift register branches and multiplied by the generator vectors

$$\mathbf{g}^1 = \left[\left(g_{0,1}^1, g_{0,2}^1, \ldots, g_{0,n_T}^1\right), \ldots, \left(g_{v_1,1}^1, g_{v_1,2}^1, \ldots, g_{v_1,n_T}^1\right)\right]$$

$$\vdots$$

$$\mathbf{g}^m = \left[\left(g_{0,1}^m, g_{0,2}^m, \ldots, g_{0,n_T}^m\right), \ldots, \left(g_{v_m,1}^m, g_{v_m,2}^m, \ldots, g_{v_m,n_T}^m\right)\right]$$

where $g_{q_i,k}^i \in \mathbb{Z}_M$, $i = 1, 2, \ldots, m$; $q_i = 0, 1, 2, \ldots, v_i$; $k = 1, 2, \ldots, n_T$. Finally, the encoder output $w_t^k \in \mathbb{Z}_M$, $t = 1, \ldots, L$; $k = 1, \ldots, n_T$, can be computed as

$$w_t^k = \left(\sum_{i=1}^{m} \sum_{q_i=0}^{v_i} \left(g_{q_i,k}^i c_{t-q_i}^k\right)\right) \bmod M. \tag{7}$$

(a)

(b)
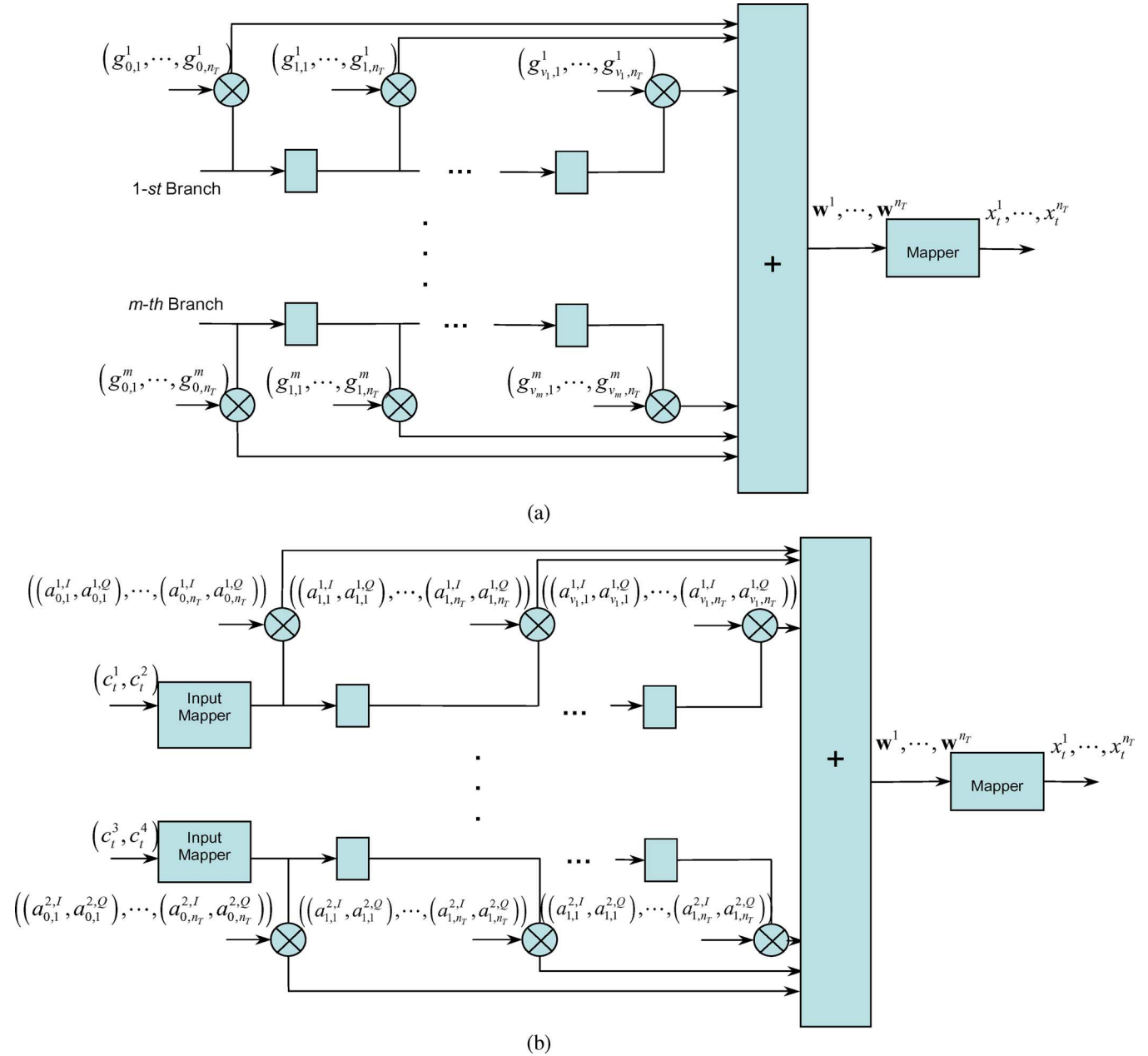
Fig. 1.   (a) M-PSK and (b) 16-QAM STTC encoder with n_T transmit antennas.

The STTC encoder can also be described in generator polynomial form. The binary input stream $\mathbf{c}^i$ can be represented as

$$\mathbf{c}^i(D) = c_0^i + c_1^i D + c_2^i D^2 + \cdots + c_t^i D^t + \cdots \qquad (8)$$

where D represents a unit delay operator. The generator matrix for antenna k can be represented as

$$\mathbf{G}_k(D) = \begin{bmatrix} \mathbf{G}_k^1(D) \\ \mathbf{G}_k^2(D) \\ \vdots \\ \mathbf{G}_k^m(D) \end{bmatrix} \qquad (9)$$

where

$$\mathbf{G}_k^i(D) = g_{0,k}^i + g_{1,k}^i D + \cdots + g_{v_i,k}^i D^{v_i} \qquad (10)$$

is the ith branch generator polynomial for transmit antenna k. The coded symbol sequence that was transmitted from antenna k is

given by

$$\mathbf{w}^k(D) = \left(\sum_{i=1}^m \mathbf{c}^i(D) \mathbf{G}_k^i(D) \right) \bmod M. \qquad (11)$$

These outputs are then mapped onto M-PSK symbols x_t^k, $t = 1, \ldots, L$; $k = 1, \ldots, n_T$, which are labeled by the integers from 0 to $M - 1$.

B. 16-QAM STTC Encoder

The 16-QAM STTC encoder with memory order v and n_T transmit antennas is shown in Fig. 1(b). At time t, the input mapper converts the input bits (c_t^1, c_t^2) and (c_t^3, c_t^4) into two components $u_t^1, u_t^2 \in \mathbb{Z}_4$, respectively, through natural mapping. The two components go through a two-branch shift register with total memory order v. The memory order of the ith branch v_i, $i = 1, 2$, is also given by (6).

The two streams of the components are multiplied by the coefficient vectors, i.e.,

$$\mathbf{g}^1 = \Big[\big(\big(a_{0,1}^{1,I}, a_{0,1}^{1,Q} \big), \ldots, \big(a_{0,n_T}^{1,I}, a_{0,n_T}^{1,Q} \big) \big), \ldots,$$

$$\big(\big(a_{v_1,1}^{1,I}, a_{v_1,1}^{1,Q} \big), \ldots, \big(a_{v_1,n_T}^{1,I}, a_{v_1,n_T}^{1,Q} \big) \big) \Big] \quad (12)$$

$$\mathbf{g}^2 = \Big[\big(\big(a_{0,1}^{2,I}, a_{0,1}^{2,Q} \big), \ldots, \big(a_{0,n_T}^{2,I}, a_{0,n_T}^{2,Q} \big) \big), \ldots,$$

$$\big(\big(a_{v_2,1}^{2,I}, a_{v_2,1}^{2,Q} \big), \ldots, \big(a_{v_2,n_T}^{2,I}, a_{v_2,n_T}^{2,Q} \big) \big) \Big] \quad (13)$$

where $a_{q_i,k}^{i,I}, a_{q_i,k}^{i,Q} \in \mathbb{Z}_4$, and $a_{j_k,i}^{k,I} + j a_{j_k,i}^{k,Q} \in \mathbb{Z}_4[j]$, $i = 1, 2$; $q_i = 0, 1, 2, \ldots, v_i$. The encoder output w_t^k, $t = 1, \ldots, L$; $k = 1, \ldots, n_T$, can be computed as

$$w_t^k = \omega_{t,k}^I + j \omega_{t,k}^Q$$
$$= \left(\sum_{i=1}^{2} \sum_{q_i=1}^{v_i} \big(a_{q_i,k}^{i,I} u_{t-q_i}^k \big) \right) + j \left(\sum_{i=1}^{2} \sum_{q_i=1}^{v_i} \big(a_{q_i,k}^{i,Q} u_{t-q_i}^k \big) \right) \bmod 4$$

where $w_t^k \in \mathbb{Z}_4[j]$. In generator polynomial form, the input components $\mathbf{u}^i$, $i = 1, 2$, can be represented as

$$\mathbf{u}^i(D) = u_0^i + u_1^i D + u_2^i D^2 + \cdots + u_t^i D^t + \cdots. \quad (14)$$

Let us define the ith branch generator polynomial for the transmit antenna k as

$$\mathbf{G}_k^i(D) = \mathbf{a}_k^{i,I}(D) + j\mathbf{a}_k^{i,Q}(D), \qquad i = 1, 2 \quad (15)$$

where $\mathbf{a}_k^{i,I}(D) = a_{0,k}^{i,I} + a_{1,k}^{i,I}D + \cdots + a_{v_i,k}^{i,I}D^{v_i}$ and $\mathbf{a}_k^{i,Q}(D) = a_{0,k}^{i,Q} + a_{1,k}^{i,Q}D + \cdots + a_{v_i,k}^{i,Q}D^{v_i}$. The generator matrix for antenna k can be represented as

$$\mathbf{G}_k(D) = \begin{bmatrix} \mathbf{G}_k^1(D) \\ \mathbf{G}_k^2(D) \end{bmatrix} = \begin{bmatrix} \mathbf{a}_k^{1,I}(D) \\ \mathbf{a}_k^{2,I}(D) \end{bmatrix} + j \begin{bmatrix} \mathbf{a}_k^{1,Q}(D) \\ \mathbf{a}_k^{2,Q}(D) \end{bmatrix}. \quad (16)$$

The coded symbol sequence transmitted from antenna k is given by

$$\mathbf{w}^k(D) = \left(\sum_{i=1}^{2} \mathbf{u}^i(D)\mathbf{G}_k^i(D) \right) \bmod 4. \quad (17)$$

The coded symbol sequence is mapped from $\mathbb{Z}_4[j]$ to a 16-QAM signal set by a *linear translation mapping* [10], i.e., $x_t^k = 2w_t^k - (3 + 3j)$.

V. NEW STTCs AND SIMULATION RESULTS

In this section, we present new sets of 4-PSK, 8-PSK, and 16-QAM STTCs for two transmit antennas over slow-fading channels. The SNR per receive antenna is defined as $\text{SNR} = n_T E_s / N_0$. We assume that each frame consists of $L = 130$ symbols and $L = 66$ symbols, for quadrature PSK and 16-QAM, respectively. This corresponds to a total of 260 and 264 information bits/frame. The coding gain of 4-PSK, 8-PSK, and 16-QAM STTCs is optimized by taking into account the first three terms of the distance spectrum in the truncated union bound (5) [10]. The coding gain $\eta(p_{\max})$ only provides an estimate of performance due to the fact that the length $p_{\max}$ that is considered in the distance spectrum is significantly less than the frame length. Therefore, after the code search, some codes will have the same diversity and gain parameters. The presented codes are the ones in

this reduced set that show the best numerical performance. Similar approaches can be found in [5], [6], and [11].

A. 4-PSK and 8-PSK STTCs

Generator coefficients are determined through exhaustive search for 4-PSK and 8-PSK signal sets. Since the encoder structure cannot guarantee geometrical uniformity of the code, the search was based on all possible pairwise error events. To reduce the complexity of the code search, we use the determinants of known codes in [5] as benchmarks. The complexity of the code search is the same as that for previously known codes reported in the literature [5], [11].

Tables I and II list the new 4-PSK and 8-PSK STTCs with bandwidth efficiency of 2 and 3 bits/s/Hz, respectively. Previously known codes are also reported for comparison. We use the standard convention of denoting the codes by the initials of the authors who proposed them. For example, we refer to the codes in [1] as "TSC." All these codes have a full rank of $r = 2$. The codes are described by memory order v; generator coefficients $\mathbf{g}^1$, $\mathbf{g}^2$; the first three minimum determinants $d_1, d_2, d_3 \in \mathcal{D}$; the associated weights $\bar{N}(d_1)$, $\bar{N}(d_2)$, and $\bar{N}(d_3)$; and the term $\eta(p_{\max})$ with $p_{\max} = 7$. Finally, SNRs at a FER of 10^{-4} with $n_R = 1, 2$ are given. In the case of $n_T = 2$, some of the known codes in Tables I and II were specifically designed for very low diversity order, i.e., $n_T n_R < 4$. We only report the corresponding SNRs for those. In all cases, we observe that the new codes have the lowest SNRs that are required to achieve the FER of 10^{-4}.

B. 16-QAM STTCs

A specific QAM rank criterion based on the linear translation mapping was first proposed in [7]. This criterion is used to determine the full-diversity 16-QAM STTCs in the $\mathbb{Z}_4[j]$ domain rather than using the complex 16-QAM signal set, so that the code search is simplified (see [7] for details). A special case of this rank criterion is described in [7, Prop. 10]. In our design, both generator matrices $\mathbf{G}_1(D)$ and $\mathbf{G}_2(D)$ in (9) have the special structure that was described in [7, Prop. 10]. Hence, the problem of determining full transmit diversity in our code search can be simplified in two steps.

Step 1) Based on [7, Prop. 10], we first check the nonsingularity of generator matrix $\mathbf{G}_1(D)$ by determining whether the polynomial $(\mathbf{a}_1^{1,I}(D)\mathbf{a}_1^{2,Q}(D)) - (\mathbf{a}_1^{2,I}(D)\mathbf{a}_1^{1,Q}(D)) \bmod 4$ has at least one odd coefficient. All the possible nonsingular generator matrices for $\mathbf{G}_1(D)$ can be also used for $\mathbf{G}_2(D)$. Remark that permutations of $\mathbf{G}_1(D)$ and $\mathbf{G}_2(D)$ are not needed since they yield an equivalent code.

Step 2) Based on [7, Prop. 10], for nonequivalent Σ_o-coefficient sets $\{\alpha_1, \alpha_2\}$ that are defined in [7, Props. 6–8], let $\mathbf{G}$ be a linear combination of the generator matrices

$$\mathbf{G} = \alpha_1 \mathbf{G}_1(D) + \alpha_2 \mathbf{G}_2(D)$$
$$= \begin{bmatrix} \hat{\mathbf{g}}^{1,I}(D) \\ \hat{\mathbf{g}}^{2,I}(D) \end{bmatrix} + j \begin{bmatrix} \hat{\mathbf{g}}^{1,Q}(D) \\ \hat{\mathbf{g}}^{2,Q}(D) \end{bmatrix} \bmod 4$$

where

$$\hat{\mathbf{g}}^{k,I}(D) = \alpha_1 \mathbf{a}_k^{1,I}(D) + \alpha_2 \mathbf{a}_k^{2,I}(D) \bmod 4,$$
$$\hat{\mathbf{g}}^{k,Q}(D) = \alpha_1 \mathbf{a}_k^{1,Q}(D) + \alpha_2 \mathbf{a}_k^{2,Q}(D) \bmod 4$$

and $k = 1, 2$. All the possible nonsingular generator matrices for $[\mathbf{G}_1(D)\mathbf{G}_2(D)]^T$ can be obtained by checking whether the polynomial $(\hat{\mathbf{g}}^{1,I}(D)\hat{\mathbf{g}}^{2,Q}(D)) - (\hat{\mathbf{g}}^{1,Q}(D)\hat{\mathbf{g}}^{2,I}(D)) \bmod 4$ has at least one odd coefficient.

If the generator matrices satisfy both conditions that were previously described, the code achieves full transmit diversity [7], and it is further

TABLE I
4-PSK STTCs

v	code	Generator Coefficients	Determinants	Weight $\bar{N}(d_i)$,	$\eta(p_{max})$ $n_R=2$	SNR (dB) FER=10^{-4}	SNR (dB) FER=10^{-4}
		$\mathbf{g}^1, \mathbf{g}^2$	d_l, d_2, d_3	$i=1,2,3$		$n_R=1$	$n_R=2$
2	[TSC]	[(0,2),(2,0)], [(0,1),(1,0)]	(4, 12, 16)	(2, 4, 1)	1.6e-1	31	18.88
	[YCVF]	[(0,2),(1,0)], [(2,2),(0,1)]	(8, 12, 20)	(3,2.12,3)	--	31	--
		[(0,2),(1,2)], [(2,3),(2,0)]	(4, 8, 12)	(0.25, 2, 0.5)	5.0e-2	--	18.3
	[JL]	[(1,2),(2,2)], [(2,1),(0,2)]	(8, 12, 16)	(1.5, 2.12, 2)	4.2e-2	30.96	18.15
	New	[(0,2),(2,1)], [(2,2),(3,2)]	(8, 12, 16)	(1.5, 2.12, 1)	4.2e-2	30.95	17.96
3	[TSC]	[(0,2),(2,0)], [(0,1),(1,0),(2,2)]	(12, 16, 20)	(2, 1, 1)	2.0e-2	30.2	17.5
	[YCVF]	[(0,2),(2,0)], [(2,1),(1,2),(0,2)]	(16, 20, 28)	(1,5,1)	--	29.91	--
		[(2,2),(2,1)], [(2,0),(1,2),(0,2)]	(8, 12, 16)	(0.5, 1, 1)	1.9e-2	--	17.35
	[LP]	[(0,2),(2,1)], [(2,0),(1,3),(0,2)]	(16, 20, 28)	(1, 3.5, 0.7)	--	29.8	--
		[(0,2),(2,2)], [(2,1),(1,1),(0,2)]	(12, 16, 20)	(0.25, 1, 1)	8e-3	--	16.84
	New	[(1,2),(2,0)], [(2,0),(3,1),(0,2)]	(16, 20, 28)	(1, 0.35, 1)	6e-3	29.69	16.6
4	[TSC]	[(0,2),(2,0),(0,2)], [(0,1),(1,2),(2,0)]	(12, 20, 28)	(1, 1.5, 3.88)	1.6e-2	29	16.75
	[YCVF]	[(0,2),(1,2),(2,2)], [(2,0),(1,1),(0,2)]	(32, 36, 44)	(2.25, 2.35, 3)	--	28.5	--
		[(1,2),(1,3),(3,2)], [(2,0),(2,2),(2,0)]	(8, 16, 24)	(0.25, 0.063, 2.56)	1.3e-2	--	16.6
	New	[(2,2),(2,1),(2,0)], [(0,2),(3,2),(2,2)]	(32, 36, 44)	(2, 2.53, 3.12)	5.5e-3	28.4	15.75
5	[YCVF]	[(2,0),(2,3),(0,2)],[(2,2),(1,0),(1,2),(2,2)]	(36, 40, 44)	(0.25, 1.53, 1.88)	--	28.2	--
		[(0,2),(2,3),(1,2)],[(2,2),(1,2),(2,3),(2,0)]	(20, 24, 28)	(0.25, 0.25, 0.5)	1.7e-3	--	15.85
	New	[(0,2),(2,1),(2,0)], [(2,2),(1,0),(1,2),(2,2)]	(36, 40, 44)	(0.006, 1.25, 1.38)	1.5e-3	28	15.5
6	[YCVF]	[(1,2),(2,2),(0,3)(2,0)],[(2,0),(2,0),(1,3),(0,2)]	(40, 48, 52)	(0.01, 0.3, 0.4)	--	26.8	--
		[(0,2),(3,1),(3,3)(3,2)],[(2,2),(2,2),(0,0),(2,0)]	(32, 40, 44)	(0.4, 0.5, 0.1)	7.5e-4	--	15.5
	New	[(2,2),(0,1),(2,0)(0,2)],[(0,2),(1,0),(1,2),(2,2)]	(48, 52, 56)	(0.3, 0.125, 1.5)	6.5e-4	26.6	15.25

TABLE II
8-PSK STTCs

v	code	Generator Coefficients	Determinants	Weight $\bar{N}(d_i)$,	$\eta(p_{max})$ $n_R=2$	SNR (dB) FER=10^{-4}	SNR (dB) FER=10^{-4}
		$\mathbf{g}^1, \mathbf{g}^2$	d_l, d_2, d_3	$i=1,2,3$		$n_R=1$	$n_R=2$
3	[TSC]	[(0,4),(4,0)], [(0,2),(2,0)], [(0,1),(5,0)]	(2, 3.37, 4)	(0.5, 0.02, 1)	0.1893	34.45	24.8
	[YCVF]	[(0,2),(2,0)], [(0,4),(4,0)], [(0,5),(1,4)]	(4, 4.34, 6.4)	(1,0.03,0.25)	--	34.1	--
		[(2,1),(3,4)], [(4,6),(2,0)], [(0,4),(4,0)]	(2,3.37,4)	(0.5,0.00165,1)	0.1876	--	20.8
	New	[(3,4),(4,1)], [(4,0),(0,4)], [(2,0),(0,6)]	(4, 4.34, 6.7)	(1,0.03,0.5)	0.07	34.0	20.45
4	[TSC]	[(0,4),(4,4)], [(0,2),(2,2)], [(0,1),(5,1),(1,5)]	(3.5,4,4.34)	(0.0156, 1, 0.0625)	0.8171	33.95	20.4
	[YCVF]	[(0,4),(4,0)], [(0,2),(2,0)], [(2,0),(6,5),(1,4)]	(4, 4.34, 5.4)	(1,0.006,0.004)	--	33.9	--
		[(2,4),(3,7)], [(4,0),(6,6)], [(7,2),(0,7),(4,4)]	(0.86, 0.9, 1.1)	(0.002, 0.008, 0.0007)	0.0132	--	20.6
	New	[(0,6),(6,0)], [(7,4),(4,0)], [(4,5),(2,1),(2,4)]	(4, 4.34, 5.86)	(0.5, 0.0009, 0.001)	0.0032	33.5	20.0
5	[TSC]	[(0,4),(4,4)],[(0,2),(2,2),(2,2)], [(0,1),(5,1),(3,7)]	(3.51,4,4.34)	(0.008, 0.25, 0.03)	0.0179	33.7	19.75
	[YCVF]	[(0,4),(4,4)],[(0,2),(2,2),(0,0)], [(3,5),(2,0),(4,0)]	(7.029,7.5,8.2)	(0.05, 0.06255, 0.094)	--	33.6	--
		[(0,4),(4,4)],[(0,2),(2,3),(2,2)], [(3,0),(2,2),(3,7)]	(2.69,3.86,4.34)	(0.25,0.0005,0.002)	0.0347	--	19.5
	New	[(4,0),(2,6)],[(7,5),(6,6),(2,2)], [(7,3),(4,6),(4,4)]	(7.5,8.0,10.8)	(0.0625, 0.0156,0.094)	0.0022	33.5	19.4

considered in the code selection. Table III lists new full-diversity 16-QAM STTCs with a bandwidth efficiency of 4 bit/s/Hz. Again, previously known codes are reported for comparison. The codes are described in the same manner as those in Tables I and II. We can again observe that the new 16-QAM codes have the lowest SNRs that are required to achieve the FER of 10^{-4}.

Let ℓ be the computation complexity of $(\mathbf{a}_i^{1,I}(D)\mathbf{a}_i^{2,Q}(D)) - (\mathbf{a}_i^{2,I}(D)\mathbf{a}_i^{1,Q}(D)) \bmod 4$ in step 1). Let n be the number of nonequivalent Σ_o-coefficient sets $\{\alpha_1, \alpha_2\}$, where $n = 2^{(2b-1)(n_T-1)}(2^{n_T} - 1) = 24$ [7], provided that $b = 2$ and $n_T = 2$. Then, in step 2), the computation complexity will be $n \times \ell$.

In our design, the code search provides saving costs of 73% and 71% of the full search by simply applying step 1) for 16-state and

64-state 16-QAM STTCs, respectively. By using Step 2), the code search provides another 8.5% and 10.5% saving costs. Note that the full-rank code search in [8] is based on Step 2) only. Hence, to search for full-rank codes, the computation complexity of our approach is only $((73\% \times \ell + 8.5\% \times n \times \ell)/(81.5\% \times n \times \ell)) = 14.12\%$ and $((71\% \times \ell + 10.5\% \times n \times \ell)/(81.5\% \times n \times \ell)) = 16.43\%$ of that in [8] for 16-state and 64-state 16-QAM STTCs, respectively.

C. Simulation Results

Fig. 2 compares the performance of the 4-PSK, 8-PSK, and 16-QAM STTCs in a multiple-antenna channel with $n_T = 2$ and $n_R = 1$. We can see that the proposed 32-state 4-PSK code outperforms

TABLE III
16-QAM STTCs

v	code	Generator Coefficients $\left(\mathbf{g}^1\right)^T, \left(\mathbf{g}^2\right)^T$		Determinants d_1, d_2, d_3	Weight $\bar{N}(d_i)$, $i=1,2,3$	$\eta(p_{max})$ $n_R=2$	SNR (dB) FER=10^{-4} $n_R=1$	SNR (dB) FER=10^{-4} $n_R=2$
2	[TSC]	$\begin{pmatrix}(0,0),(1,0)\\(3,2),(0,0)\end{pmatrix}$	$\begin{pmatrix}(0,0),(0,1)\\(2,3),(0,0)\end{pmatrix}$	(4, 5, 13)	(1.6,4,2)	0.2718	36.4	23.6
	[LFT]	$\begin{pmatrix}(3,3),(2,2)\\(2,0),(3,3)\end{pmatrix}$	$\begin{pmatrix}(1,0),(0,2)\\(0,2),(0,1)\end{pmatrix}$	(1,3,4)	(0.156,0.648,0.312)	0.2475	36.75	23.5
	[WYCKCK]	$\begin{pmatrix}(3,0),(0,2)\\(2,1),(1,1)\end{pmatrix}$	$\begin{pmatrix}(1,1),(2,1)\\(0,0),(2,1)\end{pmatrix}$	(2,6,7)	(0.337,0.0642,0.312)	0.1395	36.9	22.6
	New	$\begin{pmatrix}(0,0),(1,2)\\(3,1),(0,2)\end{pmatrix}$	$\begin{pmatrix}(2,1),(0,2)\\(2,2),(2,1)\end{pmatrix}$	(4, 5, 7)	(0.0158,0.4,0.9)	0.04	36.4	22.5
3	[WYCKCK]	$\begin{pmatrix}(2,1),(3,3)\\(0,2),(0,1)\end{pmatrix}$	$\begin{pmatrix}(0,2),(0,1)\\(0,3),(2,3)\\(3,0),(2,0)\end{pmatrix}$	(4, 5, 7)	(0.0132,0.234,0.0148)	0.0105	35.8	21.75
	New	$\begin{pmatrix}(1,0),(1,2)\\(1,1),(1,0)\end{pmatrix}$	$\begin{pmatrix}(0,1),(3,1)\\(1,0),(3,1)\\(3,1),(2,3)\end{pmatrix}$	(5, 6, 7)	(0.234,0.00098, 0.0107)	0.0096	35.4	21.6
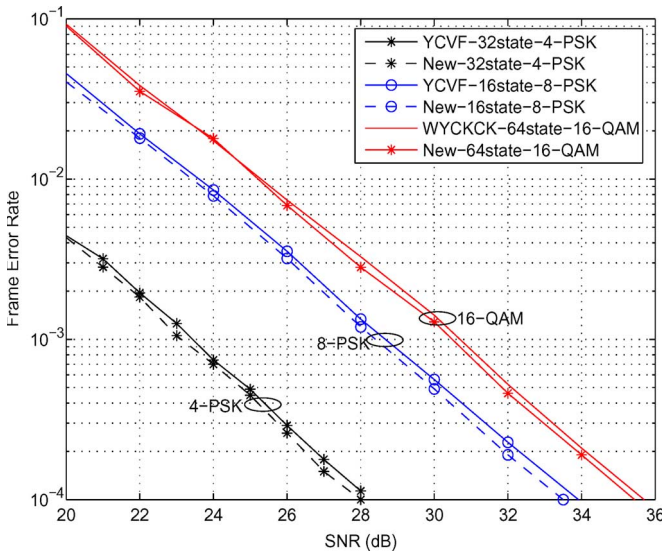
Fig. 2.   Performance of 4-PSK, 8-PSK, and 16-QAM STTCs (2Tx, 1Rx).

Fig. 3.   Performance of 4-PSK, 8-PSK, and 16-QAM STTCs (2Tx, 2Rx).

the best previously known codes by 0.2 dB at the FER of 10^{-4}. Both the new 16-state 8-PSK code and 64-state 16-QAM code outperform the current best known codes by 0.4 dB at the FER of 10^{-4}.

Fig. 3 plots the performance of 4-PSK, 8-PSK, and 16-QAM STTCs with two receive antennas over slow-fading channels. It is shown that the new 16-state 4-PSK and 8-PSK codes outperform the best previously known codes by 0.85 and 0.4 dB at the FER of 10^{-4}. It is also shown that the new 64-state 16-QAM code outperforms the current best code by 0.16 dB at the FER of 10^{-4}.

VI. CONCLUSION

Three complete sets of 4-PSK, 8-PSK, and 16-QAM STTCs over quasi-static two-antenna channels are proposed. To minimize the frame error probability, the new codes are constructed by 1) guaranteeing the codeword distance matrix to be full rank over all pairs

of codewords and 2) minimizing the gain term $\eta(p_{\max})$. Based on these design criteria, new 4-PSK and 8-PSK codes are found based on exhaustive search over the code generators. For 16-QAM STTCs, the search for full-rank codes is simplified by applying a special case of Σ_o rank criterion of [7] that saves over 80% with respect to exhaustive search. In all settings, it is shown through numerical simulations that the proposed codes outperform all previously known codes.

REFERENCES

[1] V. Tarokh, N. Seshadri, and A. R. Calderbank, "Space–time codes for high data rate wireless communication: Performance criterion and code construction," *IEEE Trans. Inf. Theory*, vol. 44, no. 2, pp. 744–765, Mar. 1998.
[2] S. Baro, G. Bauch, and A. Hansmann, "Improved codes for space–time trellis-coded modulation," *IEEE Commun. Lett.*, vol. 4, no. 1, pp. 20–22, Jan. 2000.

[3] R. S. Blum, "Some analytical tools for the design of space–time convolutional codes," *IEEE Trans. Commun.*, vol. 50, no. 10, pp. 1593–1599, Oct. 2002.

[4] D. M. Ionescu, K. K. Mukkavilli, and Z. Yuan, "Improved 8- and 16-state space–time codes for 4-PSK with two transmit antennas," *IEEE Commun. Lett.*, vol. 5, no. 7, pp. 301–303, Jul. 2001.

[5] J. Yuan, Z. Chen, B. Vucetic, and W. Firmanto, "Performance and design of space–time coding in fading channels," *IEEE Trans. Commun.*, vol. 51, no. 2, pp. 1991–1996, Dec. 2003.

[6] Y. Hong, J. Yuan, Z. Chen, and B. Vucetic, "Space–time turbo trellis codes for two, three and four transmit antennas," *IEEE Trans. Veh. Technol.*, vol. 53, no. 2, pp. 318–328, Mar. 2004.

[7] Y. Liu, M. P. Fitz, and O. Y. Takeshita, "A rank criterion for QAM space–time codes," *IEEE Trans. Inf. Theory*, vol. 48, no. 12, pp. 3062–3079, Dec. 2002.

[8] A. Wong, J. Yuan, J. Choi, S. R. Kim, I.-K. Choi, and D.-S. Kwon, "Design of 16-QAM space–time trellis codes for quasi-static fading channels," in *Proc. IEEE Veh. Technol. Conf.*, Milan, Italy, Oct. 2004, pp. 880–883.

[9] Y. S. Jung and J. H. Lee, "New measure of coding gain for space–time trellis codes," in *Proc. IEEE Int. Symp. Inf. Theory*, Washington, DC, Jun. 24–29, 2001, p. 198.

[10] D. Aktas and M. P. Fitz, "Distance spectrum analysis of space–time trellis-coded modulations in quasi-static Rayleigh-fading channels," *IEEE Trans. Inf. Theory*, vol. 49, no. 12, pp. 3335–3344, Dec. 2003.

[11] C. Liao and V. K. Prabhu, "Improved code design criteria for space–time trellis codes over quasi-static flat fading channels," in *Proc. IEEE Int. Workshop Signal Process. Advances Wireless Commun.*, New York, Jun. 2005, pp. 7–11.

Geometrically Based Statistical Channel Models for Outdoor and Indoor Propagation Environments

Lei Jiang and Soon Yim Tan, *Member, IEEE*

Abstract—This paper presents a geometrically based statistical channel model with scatterers that are randomly distributed around the base station within a circle that is determined by the coverage area of the base-station antenna. The joint probability density function (pdf) of time of arrival (TOA)/angle of arrival (AOA), the marginal pdf of AOA, and the marginal pdf of TOA are derived for a general distribution of scatterers around the base station. Rayleigh and exponential distributions are selected as special cases for discussion. Comparisons between our theoretical calculations and the empirical results, as well as the measurement data that are reported in the literature, show that the Rayleigh distribution scatterer model can be applied to an outdoor microcell propagation environment, while the exponential distribution scatterer model gives accurate results for an indoor office/laboratory propagation environment.

Index Terms—Angle of arrival (AOA), channel model, probability density function (pdf), time of arrival (TOA).

I. Introduction

In mobile communication systems, the fluctuation of the multipath propagation signal induces the fading and distortion of the received signal. To mitigate these undesirable effects, a multielement antenna is

employed at the receiver. For a smart antenna communication system, the spatial and temporal properties of the channel have an enormous impact on the performance of the system. Furthermore, in multiple-input multiple-output systems, antenna arrays are used for both the base station and the mobile receiver, and the system capacity can significantly be increased by exploiting rich multipath scattering environments. Hence, the spatial distribution of the multipath components is important in determining the system performance. Therefore, it is necessary to have channel models that can predict the angle of arrival (AOA) of multipath components and the multiple delay profile. The literature has many previous studies on such requirements [1]–[20].

The authors in [1]–[7] presented the empirical models that are derived from measurements for outdoor and indoor environments. It is found that a Gaussian probability density function (pdf) matches the azimuth pdf for the outdoor environment [2], [3], and a Laplace distribution is the best fit for the pdf of AOA for the indoor environment [5], [6]. However, empirical models are only efficient and accurate for environments with the same specific characteristics as those where the measurements were made. They cannot be used for different environments without modifications, and they are even useless when applied to quite different environments. Although both Cramer *et al.* [5] and Spencer *et al.* [6] found that the Laplace distribution is the best fit, the reported standard deviations are quite different, i.e., 38° and 25.5°, respectively. These empirical models need further modifications before they can be applied to other indoor environments.

References [8]–[20] presented analytical channel models, which are derived by assuming some ideal conditions. Among them, the single-bounce scattering geometric model is most widely used. Liberti and Rappaport [15] developed a statistical model for a microcell communication system, assuming that the scatterers are uniformly distributed inside an ellipse with foci at the base station and the mobile receiver. The circular scattering macrocell channel model [16] assumes that the scatterers are uniformly distributed within a circle around the mobile receiver, and the base station is outside this area. Ertel and Reed [12] proposed a more general approach in which the pdfs for both the elliptical [15] and circular [16] scattering models can be derived using a common approach. Olenko *et al.* [8] proposed an analytical channel model based on the assumption that omnidirectional scatterers are uniformly distributed over a 2-D hollow-disc geometry. By varying the hollow disc's thickness, this spatial density degenerates to the well-known uniform-ring or uniform-disc density [12], [16]. Despite the different geometrical shapes that are assumed in these models, distributions of the scatterers are all assumed to be uniform. The geometrical-based models for nonuniformly distributed scatterers are investigated in [13] and [18]. Janaswamy [13] presented a Gaussian scatter density model (GSDM) which assumed that the mobile station is surrounded by the scatterers of Gaussian distribution. Expressions for the pdf of the AOA, the power azimuth spectrum, the time of arrival (TOA), and the time-delay spectrum are provided. Laurila *et al.* [18] discussed the influences of different scatterer distributions on the power delay profiles and the azimuthal power spectra.

However, most of the aforementioned models are proposed to predict either macrocell or microcellular environment. Janaswamy [13] showed that GSDM is applicable to both macrocell and picocell environments by changing the value of the standard deviation (σ_s). However, a comparison with measurements showed that the performance of the model for the indoor environments is not as good as that for the outdoor environments. A simple Gaussian distribution is insufficient to model various propagation environments. In this paper, we investigate a more general situation where the distribution of scatterers can be arbitrary. The scatterers are assumed to be distributed